THE IRON-SULFUR ENVIRONMENT IN RUBREDOXIN

BRUCE BUNKER AND EDWARD A. STERN, *Department of Physics, University of Washington, Seattle, Washington 98195 U.S.A.*

ABSTRACT The atomic environment around the iron site in the nonheme iron sulfur protein rubredoxin was studied by the extended X-ray absorption fine structure (EXAFS) technique. Within experimental error, the Fe-S bonds in oxidized *Clostridium pasteurianum* rubredoxin are the same as in the analogue anion $[Fe(S_2\text{-}o\text{-xyl})_2]^-$ synthesized by Holm. The average Fe-S bond length is 2.267 ± 0.003Å and the root mean square deviation about this average due to structural disorder is $0.032\ ^{+\ 0.013}_{-\ 0.032}$.

INTRODUCTION

Recently, the extended X-ray absorption fine structure (EXAFS) near X-ray absorption edges has been shown to contain structure information (1–7). The local atomic arrangement around a particular atom type can be determined by an appropriate analysis of EXAFS. This technique is particularly applicable to metalloproteins and can complement standard diffraction methods, in that noncrystalline forms can also be studied. As one of the first applications of EXAFS to metalloproteins, the nonheme iron sulfur protein rubredoxin (8–12) (Rd) was chosen because its structure has been determined to the greatest resolution of all proteins, 1.2 Å as of now,[1] and, because, at the time with 1.5 Å resolution, the results indicated an anomalously short value of 2.05 Å for one of the Fe-S bonds (10, 13). The preparation of the rubredoxin samples has been described elsewhere (14). The 2.05 Å Fe-S distance is most unusual and it is important to check the result to determine whether any systematic error is being introduced into the X-ray diffraction technique.

Analogue compounds (15) with an Fe-S environment approximately that of Rd, yet small enough to be accurately measured by X-ray diffraction, give equal Fe-S distance within a few thousandths of an Ångstrom. Preliminary EXAFS measurements have indicated that the anomalously shortened bond does not occur (16, 17). Recent X-ray diffraction data to 1.2 Å resolution with improved analysis have also indicated that the anomalously shortened bond does not occur. The latest measured Fe-S distances[1] are 2.28, 2.28, 2.34, and 2.22 Å, which are consistent with the preliminary EXAFS results.

Recently, an exhaustive study has been made of the Rd analogues, including solution optical absorption, Mössbauer, and X-ray diffraction techniques (15). Comparing the optical and Mössbauer results led to the conclusion that the analogues have

[1]Watenbaugh, K. D., L. C. Sieker, and L. H. Jensen. Unpublished data.

an Fe-S environment similar to that of Rd but it was not possible to quantify as to how similar. Another analogue of reduced Rd has independently been synthesized (18, 19) that approximates the electronic structure of Rd even more closely than that of Holm's.

In this paper we report the results of an analysis of improved EXAFS data on oxidized *Clostridium pasteurianum* Rd, compared with various standards, including the analogues. These new results define the average Fe-S distance to be 2.267 ± 0.003 Å and indicate that the mean square radial structural disorder about this average value is $\sigma^2 = 0.001 \pm 0.001$ Å.^{2} In fact, within the accuracy of the EXAFS determination, the Fe-S environment in oxidized Rd is the same as the analogue anion (15) $[Fe(S_2\text{-}o\text{-}xyl)_2]^-$. For comparison, the corresponding results of the latest X-ray diffraction results on Rd give an average value of 2.28 Å and $\sigma^2 = 0.0018$ Å.^{2} These results are not significantly different because of the large uncertainty on the EXAFS values for σ^2.

EXAFS is an ideal tool for studying the Fe-S bonds in Rd because it can single out the Fe atom whose environment is of interest by tuning the X-ray energy to the iron's K absorption edge. These measurements can be made with equal facility on both crystalline and noncrystalline forms (2–4).

Since the EXAFS results focus on a particular atomic species and its environment, there is no chance for error from unraveling data from other parts of the molecule, as is the case with X-ray diffraction.

THEORY

The theory of EXAFS has received much attention in recent years (2, 5–7, 20, 21). The characteristic oscillations of the EXAFS are due to interference between outgoing and incoming (scattered) parts of the photoelectron excited by the absorbed X-ray photon. The scattering is by the surrounding atoms and gives information about the location of these scattering centers.

It has been shown that the EXAFS can be approximated by

$$\chi(k) = \frac{\pi m}{\hbar^2 k} \sum_j \frac{N_j t_j(2k)}{R_j^2} \sin\left[2(kR_j) + \delta_j(k))\right] \exp^{[-2(k^2\sigma_j^2 + R_j/\lambda)]}, \quad (1)$$

where $k = \sqrt{(2m/h^2)(E - E_0)}$ is the electron wave-vector, E_0 being the threshold energy for photoemission and E the X-ray photon energy. R_j is the distance to the jth shell where there are N_j scatterers. The back-scattering amplitude from atoms of the jth shell is denoted by t_j; δ_j is the phase shift of electrons scattered from the jth shell. Thermal and structural disorder is represented by σ_j, the rms deviation in bond lengths of the jth shell. The mean free path λ takes into account the finite lifetime of the final electron state.

In general, one would like to determine N_j, R_j, and σ_j from $\chi(k)$. However, detailed information about the phase shift, δ, and the threshold energy, E_0, is needed. To overcome this obstacle requires standards that sufficiently approximate the system of interest in local structure from which δ and E_0 can be calibrated. It has been shown

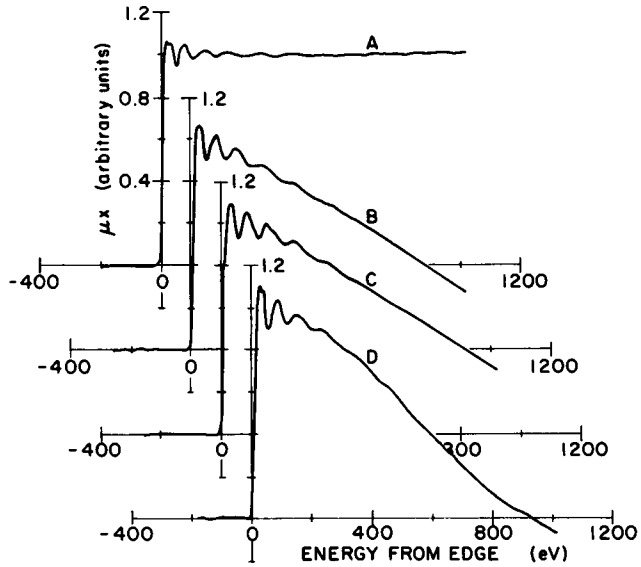

FIGURE 1 The X-ray absorption at the K-edge of iron for (A) reduced analogue, (B) oxidized analogue, (C) chalcopyrite, and (D) rubredoxin.

elsewhere (4, 22) that such a calibration is transferable for sufficiently close models. In this study, several standards were checked against one another to verify this assumption.

DATA AND RESULTS

The X-ray absorption data were taken at the Stanford Synchrotron Radiation Project, with the intense photon flux and smooth spectrum characteristic of synchrotron radiation. The apparatus has been described elsewhere.[2] Absorption spectra were taken of lyophilized Rd and compounds containing the anions

$$(Fe(S_2\text{-}o\text{-}xyl)_2]^-, \quad [Fe(S_2\text{-}o\text{-}xyl)_2]^{-2}.$$

It has been shown (15) that these anions are analogues to oxidized and reduced Rd, respectively. To test transferability of phase shifts and inner potential, data were also taken on chalcopyrite ($CuFeS_2$). Absorption spectra were taken on these compounds in the approximate energy range −200–800 eV about the iron K-edge.

The absorption spectra for Rd and the standards are shown in Fig. 1. The slow background due to processes not related to the edge have been subtracted off by the Victoreen empirical formula $\mu x = C\lambda^3 - D\lambda^4$, leaving the K-edge absorption normalized to a unit step. Near the edge fine structure can be observed due to transitions to discrete levels, as illustrated in Fig. 2 for Rd and its oxidized analogue. The first

[2]Kincaid, B. M., P. Eisenberger, and D. E. Sayers. To be published.

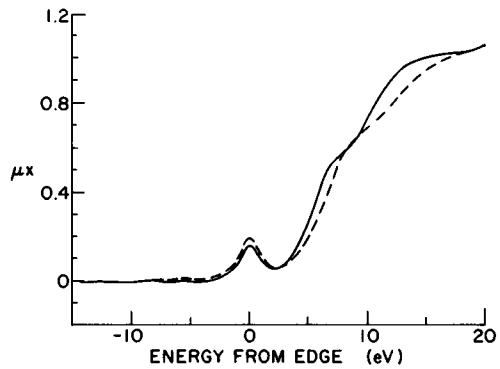

FIGURE 2 The near K-edge structure of rubredoxin (solid line) and oxidized analogue (dashed line).

"pip" is due to transitions to the unfilled 3*d*-states. At higher energies the EXAFS oscillations may be clearly seen, continuing to above 400 eV.

Fig. 3 shows the same data, but with the smooth background removed by a cubic polynomial and Fourier-filtering out low frequencies, plotted as a function of electron wave vector. The threshold energy was chosen as the 3 *d* pip below the edge. Rather than introduce a sharp cutoff in the *r*-space bandpass for filtering, we smoothly

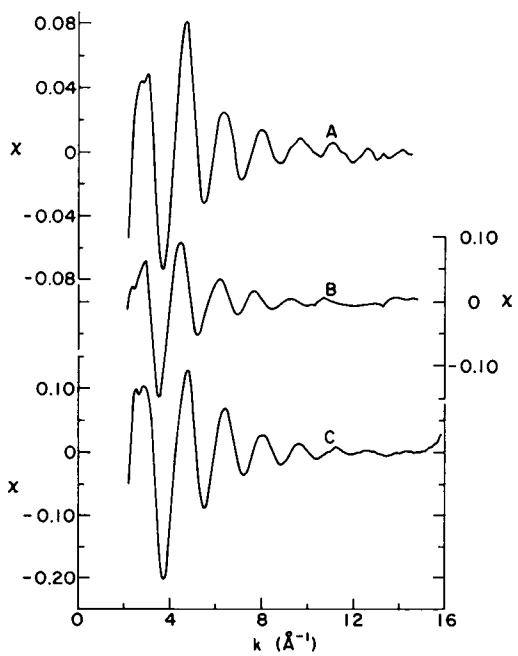

FIGURE 3 EXAFS ($\chi(k)$) plotted as a function of k for (A) rubredoxin, (B) reduced analogue, and (C) oxidized analogue.

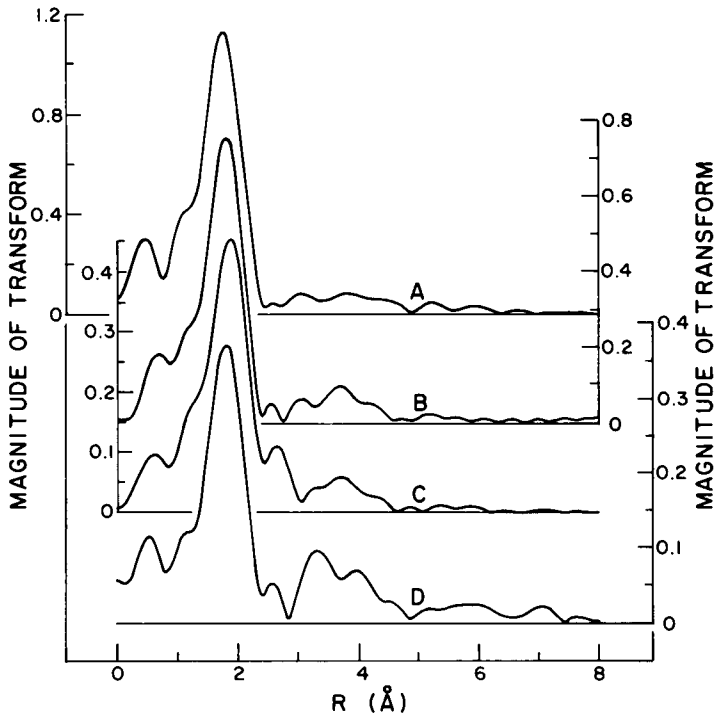

FIGURE 4 Magnitudes of Fourier transforms of $k\chi(k)$ for (A) rubredoxin (B) oxidized analogue, (C) reduced analogue, and (D) chalcopyrite.

truncate the data in r-space from 1 down to 0 Å. This procedure minimizes truncation ripple superimposed on the data. The data have all been normalized to the edge step.

Fourier transforms of the data multiplied by k are shown in Fig. 4; the data were not "massaged" in any way. The position of the transform peak is shifted from the actual distance by the average derivative $d\delta(k)/dk$ over the transform range (4). Using the known distances for the various standards, we determine the average phase shift for the system. Using this phase shift, we determine the actual distance for Rd. Table I shows peak positions, distances, and phase shifts for the various samples.

When Fourier transforming without incorporating the phase shift $\delta(k)$ in the transform, it is important to consider how the average linear phase shift enters into the transform. In particular, the envelope of the oscillations (especially as determined by the Debye-Waller factor) affects the averaging process so that disorder, both structural and thermal, must be considered when transforming. For example, the apparent phase shift of the reduced model changes about 0.01 Å between the room temperature and low temperature data because of the Debye-Waller factor, while the phase shifts for the oxidized and reduced models at the same temperature are consistent with one another to within 0.003 Å.

To interpret the disorder results, it is necessary to separate the disorder into its

TABLE I

Fe-S DISTANCES

Sample	EXAFS peak position	Actual distance	Phase shift
		Å	
Oxidized analogue	1.784 ± 0.0025	2.267*	0.4830 ± 0.0025
Reduced analogue	1.873 ± 0.004	2.356*	0.4827 ± 0.004
Chalcopyrite	1.801 ± 0.001	2.269*	0.4680 ± 0.001
Rubredoxin	1.785 ± 0.002	2.267 ± .003‡	

*Distance from diffraction data.

‡Distance found by using oxidized analogue phase shift.

structural and thermal components. By structural disorder, we mean the deviation of the average bond length for a given Fe-S pair from the mean value of the four Fe-S bonds. The thermal disorder is caused by thermal vibrations varying the length of the Fe-S bond about its median value, i.e., the stretching mode of oscillation.

It is reasonable to assume that thermal vibrations cause the Fe-S bond lengths to have a Gaussian distribution

$$P(u) = (2\pi\sigma^2)^{-1/2} e^{-u^2/2\sigma^2}, \tag{2}$$

where $P(u)du$ is the probability that the bonds deviate from their average by a value in the range $[u, u + du]$. Such a variation leads to the Debye-Waller type factor $\exp(-2\sigma^2k^2)$ of Eq. 1 (4).

If the average values of the Fe-S bond lengths are not all equal but differ by a small amount (structural disorder), then it is simple to show that the Debye-Waller factor of Eq. 1 is replaced by

$$(1 - 2k^2\sigma_s^2)e^{-2k^2\sigma_T^2}, \ (2k^2\sigma_s^2 \ll 1), \tag{3}$$

where σ_s^2 is the mean square deviation from the mean Fe-S bond length due to structural disorder, and σ_T^2 is the mean square deviation due to thermal vibration in the stretching mode including zero point motion. The result in Eq. 3 is independent of the form of the structural disorder as long as $k^2\sigma_s^2 \ll 1/2$.

If $\chi(k)$ is dominated by one shell or if a given shell is isolated by Fourier filtering, then $\chi(k)$ would have an oscillation amplitude of the form

$$\chi(k) = Bt(2k)(1 - 2k^2\sigma_s^2)e^{-2k^2\sigma_T^2}, \tag{4}$$

where B is independent of k.

If such a spectrum is compared with a standard with the same $t(2k)$, the ratio of the standard's $\chi_1(k)$ to that of the sample's $\chi_2(k)$ is

$$\ln[\chi_1(k)/\chi_2(k)] = 2k^2[\sigma_{2s}^2 - \sigma_{1s}^2) + (\sigma_{2T}^2 - \sigma_{1T}^2)] + \text{const.} \tag{5}$$

Thus, a plot of the left side of Eq. 5 vs. k^2 should be a straight line with slope propor-

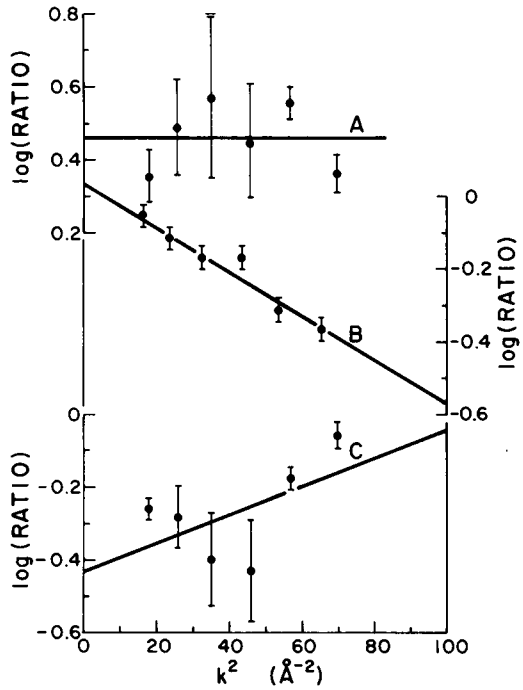

FIGURE 5 The $\ln[\chi_1(k)/\chi_2(k)]$ vs. k^2 for (A) rubredoxin (293°K)/ reduced analogue (293°K), (B) reduced analogue (293°K)/ reduced analogue (120°K), and (C) reduced analogue (120°K)/ oxidized analogue (120°K). Also plotted are the least-square fits to the data.

tional to the difference in the total mean square disorder, both structural and thermal, between the standard and the sample. In order to separate σ_T from σ_s, one ideally measures the temperature dependence of the sample and the standard.

Fig. 5 shows plots of Eq. 5 for rubredoxin (room temperature)/reduced analogue (room temperature; reduced analogue (room temperature)/reduced analogue (low temperature); and reduced analogue (room temperature)/oxidized analogue (low temperature). Table II shows derived disorder parameters for the various samples. [Error bars in $\Delta\sigma^2$ are estimated as indicated in the Discussion and Conclusion section of this paper.] From diffraction data, it is known that the structural disorder for the reduced analogue is $\sigma^2 = 0.0005$ and we estimate that the $\Delta\sigma_T^2 = 7.5 \times 10^{-4}$ as discussed at the end of this section. These numbers and the results of Table II lead to a value for Rd of $\sigma_s^2 = 0.001 \pm 0.001$ or $\sigma_s = 0.032 \begin{matrix} +0.013 \\ -0.032 \end{matrix}$.

We successfully managed to measure the temperature dependence of only the reduced analogue to Rd. For the other samples, including Rd, we obtained usable data at only one temperature. In analyzing our data we assumed that Rd has the same temperature dependence as the oxidized analogue. This assumption is supported by the fact that the average thermal vibration amplitudes of both reduced and oxidized analogues from X-ray diffraction are within 10% of each other at room temperature

TABLE II

RELATIVE RADIAL DISORDER

$\sigma^2(B') - \sigma^2(B)$	0.003 ± 0.0003
$\sigma^2(A) - \sigma^2(B')$	0.000 ± 0.001
$\sigma_T^2(A) - \sigma_T^2(B')$	0.00075
$\sigma_s^2(B')$	0.0005
$\sigma_s^2(A)$	0.001 ± 0.001
$\sigma_s(A)$	$0.032^{+0.013}_{-0.032}$

Sample B', reduced analogue (293°K); B, reduced analogue (120°K); A, rubredoxin (293°K). σ^2, total disorder, $\sigma_T^2 + \sigma_s^2$; σ_T^2, thermal disorder; σ_s^2, structural disorder, rms deviation in Fe-S bond lengths from average value.

(Tables III and IV) showing that the thermal vibration effects are not too sensitively dependent on the Fe-S environment. EXAFS measures only the vibrations averaged over the various bond lengths, and is not sensitive to anisotropies in the vibrations. We show experimentally that Rd has the same average Fe-S bond lengths as the oxidized analogue, which is 0.09 Å shorter than that of the reduced analogue, and thus it is reasonable to assume that their thermal vibrations are similar.

It is important to note that the σ_T determined by EXAFS is different from that determined by X-ray diffraction, which yields much larger values. The σ_T of EXAFS is the relative radial disorder in the Fe-S bond, while the X-ray diffraction results reflect the displacement from the average position of a given atom. If the radial bonds between Fe-S atoms are rigid but the whole complex vibrates about an average position and pivots about the Fe center, it is possible for the diffraction σ to be much larger than the EXAFS result, as is the case for the Rd analogues.

To check consistency between our results and those of diffraction, we have computed the rms amplitudes of vibration for the Fe and S atoms along the Fe-S directions as derived from diffraction data (15). The difference between the rms amplitudes for Fe and S gives a lower bound for what EXAFS should measure in terms of radial

TABLE III

RMS AMPLITUDES OF VIBRATION ALONG Fe-S BOND DIRECTION FOR $Na(Ph_4AS)[Fe(S_2\text{-}o\text{-}xyl)_2]$ (REDUCED ANALOGUE) AS DERIVED FROM DIFFRACTION DATA OF REF. 12

Fe-S bond	$\sigma_{rms}(Fe)$	$\sigma_{rms}(S)$	$\lvert \sigma_{rms}(Fe) - \sigma_{rms}(S) \rvert$
1	0.189 ± 0.004	0.198 ± 0.006	0.009 ± 0.010
2	0.247 ± 0.004	0.249 ± 0.007	0.001 ± 0.011
3	0.234 ± 0.004	0.241 ± 0.006	0.007 ± 0.010
4	0.310 ± 0.004	0.306 ± 0.006	0.004 ± 0.010
Average	0.245 ± 0.0023	0.249 ± 0.004	0.005 ± 0.006

TABLE IV

RMS AMPLITUDES OF VIBRATION ALONG Fe-S BOND DIRECTION FOR $(Et_4N)[Fe(S_2\text{-}o\text{-}xyl)_2]$ (OXIDIZED ANALOGUE) AS DERIVED FROM DIFFRACTION DATA OF REF. 12

Fe-S bond	σ_{rms}(Fe)	σ_{rms}(S)	$\lvert\sigma_{rms}(Fe) - \sigma_{rms}(S)\rvert$
1	0.210 ± 0.001	0.223 ± 0.002	0.013 ± 0.003
2	0.217 ± 0.001	0.222 ± 0.002	0.003 ± 0.003
3	0.246 ± 0.001	0.238 ± 0.002	0.008 ± 0.003
4	0.248 ± 0.001	0.220 ± 0.002	0.028 ± 0.003
Average	0.230 ± 0.0006	0.226 ± 0.0012	0.013 ± 0.002

disorder, and indeed, this limit is consistent with our results. The results for the reduced and oxidized analogues are summarized in Table III and Table IV, respectively.

In separating out thermal and structural disorder, we must estimate the vibration contribution to σ^2 at room temperature for the reduced analogue, using its measured temperature dependence listed in Table II. To do so, we assume the stretching mode has a single frequency ω, in which case it is easy to show that the difference between the mean square amplitude of vibration at temperatures T_1 and T_2 is

$$\Delta\sigma^2 = \frac{\hbar}{2\omega m}\left[\frac{1}{(e^{\hbar\omega/k_BT_1}) - 1} - \frac{1}{(e^{\hbar\omega/k_BT_2}) - 1}\right]. \tag{7}$$

We are interested in the mode where the center of mass of the system is fixed and only the S atom is moving, so that we set m equal to the mass of S.

Using the value of $\Delta\sigma^2$ from the reduced analogue (293°K and 120°K), we find that $\hbar\omega = 0.017$ eV. Substituting this value in the expression

$$\sigma^2 = \frac{\hbar^2}{2m\omega}\left(\frac{1}{e^{\hbar\omega/k_BT} - 1} + \frac{1}{2}\right), \tag{8}$$

we have σ^2 thermal = $(0.062)^2$Å^2 and σ^2 zero point = $(0.035)^2$Å^2 and σ(293°C) = 0.07 Å. The zero point contribution comes from the term $\frac{1}{2}$ in the parenthesis of Eq. 8. Although these values are approximate, they do give a good idea of the size of the effects being considered. We note from Tables III and IV that the reduced analogue has about a 7.5% larger average σ than the oxidized analogue. It is reasonable to expect that the reduced analogue will have a weaker restoring force, since its Fe-S bond length is increased. Assuming that this same percentage difference occurs in the EXAFS σ, one expects a 15% difference in $\sigma_T^2(A) - \sigma_T^2(B) = 0.15\ (0.07)^2$, as presented in Table II.

DISCUSSION AND CONCLUSIONS

The results obtained on *Clostridium pasteurianum* Rd presented here give an indication of the accuracy and information available from EXAFS measurements on metalloproteins. The ability to measure average distances to a few thousands of an Ångstrom is

possible if care is taken. The standard against which the sample is compared must approximate it rather closely. The Rd analogues of Holm (15) served that purpose here. Not only must the surroundings be similar in both the sample and standard but their disorder (both thermal and structural) must also be similar.

We have shown that the analogues of Holm (15) have the same Fe-S bond lengths as Rd to within our uncertainties. Yet there are differences in the electronic properties between the analogues and Rd. These are visible in our near-edge X-ray absorption spectra (Fig. 2) and in the optical solution absorption spectra (15). One of the reduced analogues of ref. 16 more closely approximates the Mössbauer spectra of Rd than does that of Holm. The average Fe-S bond length is the same within 0.001 Å in the two analogues but the distribution of the bond lengths differ. The Holm reduced analogue has a $\sigma_s = 0.022$ while that of ref. 16 has $\sigma_s = 0.012$. The relation between atomic structure and the absorption spectra is indirect and it is clear from the results on Rd and the analogues that it is not possible at present to reliably relate the spectra differences to structure differences. It appears in these cases that the structure differences that produce the spectra differences occur either outside the Fe-S complex, or else the spectra are extremely sensitive to very small structural differences.

What has been a disappointment is the large uncertainty in the disorder parameter σ, an order of magnitude larger than the uncertainty in the average value. This uncertainty is larger than that predicted from random noise in the data and must be caused by systematic errors or a breakdown in the theoretical assumptions. The errors shown in Fig. 5 reflect both the systematic and random errors. The random errors are smaller and represent the fluctuation when a measurement is immediately repeated. In addition to this source of error, there are also systematic errors associated with correctly subtracting the smooth background from the EXAFS. This problem with background is affected by sample position in the beam, the position of the electron beam in the storage ring, imperfections in the monochromating crystal, etc.

The plots of Fig. 5 are predicted theoretically to be straight lines under the following assumptions: $2k^2\sigma^2 \ll 1$; and $t(2k)$ and $\lambda(k)$ did not change. The backward scattering amplitude $t(k)$ depends somewhat on the charge distribution around the scattering atom and this should affect mostly the low k values. There are also some systematic errors that could be introduced at low k in analyzing the data. However, the plots of Fig. 5 do not seem to have their deviation from a straight line located only at low k. Many body effects,[3] neglected in Eq. 1, may also possibly make varying k-dependent contributions from sample to standard. The importance of many-body effects has not been explored in much detail. The dependence of $\lambda(k)$, also mainly a many-body effect, has also not been explored in any detail.

It's useful to point out a limitation of EXAFS in determining the disorder in a given shell. When $2k^2\sigma^2 \ll 1$, as was the case here, one cannot determine the configuration of the distribution of the atoms about the average position. Only one pa-

[3]Martin, R. M., J. J. Rehr, E. Davidson, and E. A. Stern. Unpublished data. P. A. Lee. Unpublished data.

rameter can be determined, i.e., σ. The information to distinguish different distributions can be discerned only if $k^2\sigma^2 \geq 1$.

Using the distribution of bond lengths suggested by X-ray diffraction results on Rd, we can translate our results into the diffraction results. First we assume one of the Fe-S bonds is shortened while the other three are the same, as suggested by the analysis of the 1.5 Å resolution diffraction data (10). In this case our results imply three S atoms all at the same distance, somewhere in the range 2.267–2.292 Å, and the shortened bond somewhere between 2.267–2.189 Å. The range is due to our uncertainty. Next we assume that two of the bonds are equal to the average value while one bond is shortened and the other lengthened about the average, as indicated by the 1.2 Å resolution data.[1] In this case our results imply two S atoms at 2.267 Å, one somewhere between 2.267 and 2.203 Å and the other between 2.267 and 2.331 Å. In all cases the atom positions must be correlated so that their average distance is 2.267 ± 0.003.

Taking into account the systematic and random errors present in the X-ray diffraction data, the latest diffraction results[1] for the Fe-S bonds of 2.22, 2.34, 2.28, and 2.28 Å are consistent with the values presented in the second case just above. The average value of the bonds are determined more accurately by EXAFS than by X-ray diffraction. However, the exact configuration of the distribution of the bond lengths about their average cannot be determined by EXAFS in this case, since the useful data are in the range where $k^2\sigma^2 < \frac{1}{2}$, and only σ can be determined. Even the value of σ cannot be determined with as much precision as the random noise in the data implies. The reason for this is not presently understood. However, considering that EXAFS is only a few years in development, it is reasonable to expect that with more experience the full potential of EXAFS will be realized.

The constant advice of and informative discussions with Profs. Lyle Jensen and William W. Parson are gratefully acknowledged. We are most indebted to Professor R. Holm, who kindly supplied both his oxidized and reduced analogues of Rd, and to Dr. Walter Lovenberg, who kindly supplied the Rd samples. We are particularly indebted to Prof. Jon Herriott, who first pointed out the appropriateness of measuring Rd and who helped obtain the samples. Prof. Dale Sayers and Dr. Steve Heald helped in the measurements. The use of the superb facilities at the Stanford Synchrotron Radiation Project and the excellent support given by their personnel were essential for the success of the measurements.

Research supported by the National Science Foundation Grants DMR73-02521 and DMR73-07692 in cooperation with SLAC and the U.S. Energy Research and Development Administration.

Received for publication 11 March 1977.

REFERENCES

1. SAYERS, D. E., E. A. STERN, and F. W. LYTLE. 1971. New technique for investigating non-crystalline structures: Fourier analysis of the extended X-ray absorption fine structure. *Phys. Rev. Lett.* **27**:1204.
2. STERN, E. A. 1974. Theory of the extended X-ray absorption fine structure. *Phys. Rev. B.* **10**:3027.
3. LYTLE, F. W., D. E. SAYERS, and E. A. STERN. 1975. The EXAFS technique. II. Experimental practice and selected results. *Phys. Rev. B.* **11**:4825.
4. STERN, E. A., D. E. SAYERS, and F. W. LYTLE. 1975. The EXAFS technique. III. Determination of physical parameters. *Phys. Rev. B.* **11**:4836.

5. LEE, P. A., and J. B. PENDRY. 1975. Theory of the extended X-ray absorption fine structure. *Phys. Rev. B.* **11**:2795.
6. LEE, P. A., and G. BENI. 1976. A new method for calculation of atomic phase shifts. Application to the extended X-ray absorption fine-structure (EXAFS) in molecules and crystals. *Phys. Rev. B.* In press.
7. ASHLEY, C. A., and S. DONIACH. 1975. Theory of extended X-ray absorption fine structure (EXAFS) in crystalline solids. *Phys. Rev. B.* **11**:1279.
8. ORME-JOHNSON, W. H. 1973. Iron-sulfur proteins: structure and function. *Annu. Rev. Biochem.* **42**: 159.
9. PALMER, G. 1975. Iron-Sulfur Proteins. *Enzymes.* **12**:2.
10. JENSEN, L. H. 1974. X-ray structural studies of ferredoxin and related electron carriers. *Annu. Rev. Biochem.* **43**:461.
11. EATON, W. A., and W. LOVENBERG. 1973. The iron-sulfur complex in rubredoxin. *In* Iron-Sulfur Proteins. W. Lovenberg, editor. Academic Press, Inc., New York. **2**:131.
12. LOVENBERG, W. 1974. Ferrodoxin and rubredoxin. *In* Microbial Iron Metabolism. J. B. Neilands, editor. Academic Press, Inc., New York. 161.
13. WATENBAUGH, K. D., L. C. SIEKER, J. R. HERRIOT, and L. H. JENSEN. 1973. Refinement of the model of a protein: rubredoxin at 1.5 Å resolution. *Acta Crystallogr. Sect. Struct. Crystallogr. Cryst. Chem.* **29**:943.
14. LOVENBERG, W., and B. E. SOBEL. 1965. Rubredoxin: A new electron transfer protein from *Clostridium pasteurianum. Proc. Natl. Acad. Sci. U.S.A.* **54**:193.
15. LANE, R. W., J. A. IBERS. 1974. Synthetic analogues of the active sites of iron-sulfur proteins. XIV. Synthesis, properties, and structures of BIS(*o*-xylyl-α,α'-DITHIOLATO) ferrate(II,III) anions, analogs of oxidized and reduced rubredoxin sites. *J. Am. Chem. Soc.* **99**:84.
16. SAYERS, D. E., E. A. STERN, and J. R. HERRIOT. 1976. Measurement of Fe-S bond lengths in rubredoxin using extended X-ray absorption fine structure (EXAFS). *J. Chem. Phys.* **64**:427.
17. SHULMAN, R. G., P. EISENBERGER, W. E. BLUMBERG, and N. A. STOMBAUGH. 1975. Determination of the iron-sulfur distances in rubredoxin by x-ray absorption spectroscopy. *Proc. Natl. Acad. Sci. U.S.A.* **72**:4003.
18. SWENSON, D., N. C. BAENZIGER, D. G. HOLAH, A. KOSTIKAS, A. SIMOPOULUS, and V. PETROULEAS. 1976. The crystal and molecular structures of $[(C_6H_5)_4P]_2$ $Fe(S_2C_4O_2)_2$ and $[(C_6H_5)_4P]_2$ $Fe(SC_6H_5)_4$, a structural analogued reduced rubredoxin. *J. Am. Chem. Soc.* **98**:5721.
19. KOSTIKAS, A., V. PETROULEAS, A. SIMPOULOS, D. COUCOUVANIS, and D. G. HOLAH. 1976. Mössbauer effect in synthetic analogs of rubredoxin. *Chem. Phys. Lett.* **38**:582.
20. REHR, J. J., and E. A. STERN. 1976. Multiple scattering corrections to the extended X-ray absorption fine-structure. *Phys. Rev. B.* **14**:4413.
21. SCHAICH, W. L. 1976. Theory of extended X-ray absorption fine structure: one-dimension model calculations. *Phys. Rev. B.* **14**:4420.
22. CITRIN, P. H., P. EISENBERGER, and B. M. KINCAID. 1976. Transferability of phase shifts in extended X-ray absorption fine structure, *Phys. Rev. Lett.* **36**:1346.